

Noname manuscript No.
(will be inserted by the editor)

A quadratic optimization program for the inverse elastography problem

Sílvia Barbeiro · Rafael Henriques ·
José Luis Santos

Received: date / Accepted: date

Abstract In this work we focus on the development of a numerical algorithm for the inverse elastography problem. The goal is to perform an efficient material parameter identification knowing the elastic displacement field induced by a mechanical load. We propose to define the inverse problem through a quadratic optimization program which uses the direct problem formulation to define the objective function. In this way, we end up with a convex minimization problem which attains its minimum at the solution of a linear system. The effectiveness of our method is illustrated through numeral examples.

Keywords linear elasticity · inverse problem · mechanical properties reconstruction · optimization problem

1 Introduction

Optical coherence elastography (OCE) is an emerging biomedical imaging technique based on the optical coherence tomography (OCT) imaging modality to form pictures of biological tissue and map its biomechanical properties. An acoustic excitation system can be used for inducing a mechanical load to the tissue leading to a deformation response. OCE combines the mechanical excitation with OCT for measuring the corresponding elastic displacement [6, 10, 12, 14].

Sílvia Barbeiro
University of Coimbra, Department of Mathematics, CMUC, 3000-143 Coimbra, Portugal
E-mail: silvia@mat.uc.pt

Rafael Henriques
University of Coimbra, Department of Mathematics, CMUC, 3000-143 Coimbra, Portugal
E-mail: rafael.henriques@mat.uc.pt
Corresponding author

José Luis Santos
University of Coimbra, Department of Mathematics, CMUC, 3000-143 Coimbra, Portugal
E-mail: zeluis@mat.uc.pt

The main goal of this paper is to propose a method to obtain the mechanical properties of a medium given the displacement field for a given excitation, that is, to solve the inverse problem of elastography. The predominant approaches in the literature are based on minimizing the difference between the measured and simulated displacements (*e.g.* [7, 11, 13]). Differently, in our method, we use the direct problem to define the objective function. In particular, we compute the parameters that characterize the mechanical properties of the medium such that the given data solves the direct problem. The advantage is that, in our case, we end up with a convex objective function.

In both, the direct and the inverse problems, we consider the medium as a material with linear isotropic mechanical behavior, purely elastic.

We will work with the displacement field defined on piecewise linear function spaces which is a common simple choice for the basis functions when using the finite element method (FEM). For the case of a nearly incompressible materials, *i.e.* with Poisson's ratio ν close to 0.5, the performance of a classical FEM scheme can deteriorate due to locking as $\nu \rightarrow 0.5$ [1]. Here we are assuming that we are dealing with media for which the range of values of the Poisson's ratio leads to locking-free FEM solutions. As an example of application, we can mention the aortic elastography [8]. Concerning materials for which locking is an issue, some numerical methods have been proposed in the literature, in particular some variations of mixed finite element methods [5].

The article is organized as follows. In Section 2 we describe the mathematical model for the direct problem. We consider time-harmonic equations of linear elasticity and we derive the corresponding numerical solution using continuous piecewise linear finite elements in a three-dimensional domain. The numerical method for this direct problem is the computational basis to address the inverse problem. In Section 3 we propose and analyse the convex optimization problem through which we intend to infer the mechanical properties of the medium knowing the induced deformations. Finally, in Section 4 we present several computational results including simulations with noise free data and noisy data.

2 Elasticity model

2.1 The time-harmonic formulation

We start by considering a mathematical model for the mechanical deformation as it is presented in [3]. This direct problem will be formulated grounded on well-established physical laws, which provide equations that relate the biomechanical properties to the measured mechanical response. Our model is based on equations for linear elasticity and we assume that mechanical behavior of the medium is purely elastic and isotropic. Considering time-harmonic excitations in the linear elasticity model, the displacement field is assumed to have a time-harmonic form [2, 7].

To derive the mathematical model, we begin by introducing some notation needed. Let p be a scalar function, $\mathbf{v} = (v_i)_{1 \leq i \leq 3}$ a vector function and $\mathbf{A} = (a_{ij})_{1 \leq i, j \leq 3}$ a matrix of functions of three variables, all defined in a bounded domain $\Omega \subset \mathbb{R}^3$. We also make use of the following Lebesgue spaces

$$L^2(\Omega) = \{\mathbf{v} : \|\mathbf{v}\|_{L^2(\Omega)} < \infty\}, \quad L^2(\Omega) = \{\mathbf{A} : \|\mathbf{A}\|_{L^2(\Omega)} < \infty\},$$

where

$$\|\mathbf{v}\|_{L^2(\Omega)} = (\mathbf{v}, \mathbf{v})_{L^2(\Omega)}^{1/2}, \quad \|\mathbf{A}\|_{L^2(\Omega)} = (\mathbf{A} : \mathbf{A})_{L^2(\Omega)}^{1/2},$$

endowed with the inner products defined by

$$(\mathbf{u}, \mathbf{v})_{L^2(\Omega)} = \int_{\Omega} \mathbf{u} \cdot \mathbf{v} \, dx = \sum_{i=1}^3 \int_{\Omega} u_i v_i \, dx,$$

$$(\mathbf{A} : \mathbf{B})_{L^2(\Omega)} = \int_{\Omega} \mathbf{A} : \mathbf{B} \, dx = \sum_{1 \leq i, j \leq 3} \int_{\Omega} a_{ij} b_{ij} \, dx.$$

The space

$$H^1(\Omega) = \{\mathbf{u} : \mathbf{u} \in L^2(\Omega) \wedge \nabla \mathbf{u} \in L^2(\Omega)\}$$

is equipped with the following inner product

$$(\mathbf{u}, \mathbf{v})_{H^1(\Omega)} = (\nabla \mathbf{u} : \nabla \mathbf{v})_{L^2(\Omega)} + (\mathbf{u}, \mathbf{v})_{L^2(\Omega)}.$$

Now let us consider an isotropic elastic material in the configuration space $\Omega \subset \mathbb{R}^3$, where Ω is a polyhedron with boundary $\partial\Omega$. Given a distribution of body forces \mathbf{f} , we intend to characterize the field of induced displacements $\mathbf{u}(x, t)$ through the space Ω and time \mathbb{R}_0^+ .

In the case of a sinusoidal excitation, as in the acoustic case, the displacement field has a time-harmonic form given by [7]

$$\mathbf{u}(x, t) = \Re(\mathbf{u}(x) e^{i\omega t}),$$

where \Re denotes the real part of a complex and ω is the angular frequency of the sinusoidal excitation. In this case, the elastic displacement field \mathbf{u} satisfies the Lamé equation

$$\mu \nabla^2 \mathbf{u} + (\lambda + \mu) \nabla(\nabla \cdot \mathbf{u}) + \omega^2 \rho \mathbf{u} + \mathbf{f} = 0 \text{ in } \Omega \quad (1)$$

where ρ is the material density. The Lamé constants, μ and λ , are given by

$$\mu = \frac{E}{2(1+\nu)} \text{ and } \lambda = \frac{\nu E}{(1+\nu)(1-2\nu)},$$

where E, ν are the Young's Modulus and the Poisson's ratio, respectively.

Equation (1) is complemented with boundary conditions. Let Γ_1 and Γ_2 be two open subsets of $\partial\Omega$ such that $\partial\Omega = \bar{\Gamma}_1 \cup \bar{\Gamma}_2$, $\Gamma_1 \cap \Gamma_2 = \emptyset$ and $\text{meas}(\Gamma_2) > 0$. Considering the strain tensor $\varepsilon(\mathbf{u}) = \frac{1}{2}(\nabla \mathbf{u} + (\nabla \mathbf{u})^\top)$, the stress tensor $\sigma(\mathbf{u}) = 2\mu \varepsilon(\mathbf{u}) + \lambda \text{tr}(\varepsilon(\mathbf{u}))\mathbf{I}$ (where $\text{tr}(\cdot)$ and \mathbf{I} denote the trace of the matrix and the

3×3 identity matrix, respectively) and \mathbf{n} the unit outer normal direction, we impose the traction boundary condition

$$\sigma(\mathbf{u})\mathbf{n} = \mathbf{g} \text{ on } \Gamma_1, \quad (2)$$

and the displacement boundary condition

$$\mathbf{u} = 0 \text{ on } \Gamma_2. \quad (3)$$

2.2 The finite element method

In this section we briefly introduce the finite element method associated to the mathematical model (1)–(3) (see *e.g.* [4]) which we will develop in its matrix form in Section 2.4, in order to solve the inverse problem. We start by considering the weak form of this model. Let

$$V = \{\mathbf{v} \in H^1(\Omega) : \mathbf{v}|_{\Gamma_2} = 0\}. \quad (4)$$

The weak formulation of (1)–(3) reads: find $\mathbf{u} \in V$ such that

$$a(\mathbf{u}, \mathbf{v}) = l(\mathbf{v}), \quad \forall \mathbf{v} \in V, \quad (5)$$

where

$$a(\mathbf{u}, \mathbf{v}) = \int_{\Omega} 2\mu \varepsilon(\mathbf{u}) : \varepsilon(\mathbf{v}) + \lambda(\nabla \cdot \mathbf{u})(\nabla \cdot \mathbf{v}) - \omega^2 \rho \mathbf{u} \cdot \mathbf{v} \, dx \quad (6)$$

and

$$l(\mathbf{v}) = \int_{\Gamma_1} \mathbf{g} \cdot \mathbf{v} \, ds + \int_{\Omega} \mathbf{f} \cdot \mathbf{v} \, dx.$$

Here we are assuming that $\mathbf{g} \in L^2(\Gamma_1)$ and $\mathbf{f} \in L^2(\Omega)$.

Let us consider a partition of Ω into M tetrahedra K_j , $j \in \{1, \dots, M\}$ such that

$$\Omega = \bigcup_{j=1}^M K_j.$$

The resulting partition is denoted by Ω_h where h represents its diameter. For any pair of tetrahedra in the partition K_i and K_j , $i \neq j$, $K_i \cap K_j$ is either empty, or a common vertex, edge or face of K_i and K_j .

Let us consider the finite dimensional subspace $V_h \subset V$ of continuous piecewise linear functions on each tetrahedron. Assuming that N is the total number of vertices associated with the tetrahedra in Ω_h then $\dim V_h = 3N$. The finite element formulation of the problem (5) consist of finding $\mathbf{u}_h \in V_h$ such that

$$a(\mathbf{u}_h, \mathbf{v}_h) = l(\mathbf{v}_h), \quad \forall \mathbf{v}_h \in V_h. \quad (7)$$

2.3 Well-posedness

Let us discuss the existence and uniqueness of solutions of problems (5) and (7).

Applying the Riesz-Schauder theory [9, Theorem 6.5.15] we derive the following result.

Lemma 1 *Let $a(\cdot, \cdot)$ be a V -coercive bilinear form such that*

$$a(\mathbf{u}, \mathbf{v}) = b(\mathbf{u}, \mathbf{v}) + \beta_1(\mathbf{u}, \mathbf{v})_{L^2(\Omega)},$$

being $b(\cdot, \cdot)$ a V -elliptic bilinear form. For each $\beta_1 \in \mathbb{C}$ we have one of the following alternatives:

1. *the problem $a(\mathbf{u}, \mathbf{v}) = l(\mathbf{v})$ has a unique solution;*
2. *β_1 is an eigenvalue of the problem.*

Defining

$$b(\mathbf{v}, \mathbf{v}) = \int_{\Omega} 2\mu\varepsilon(\mathbf{v}) : \varepsilon(\mathbf{v}) + \lambda(\nabla \cdot \mathbf{v})^2 dx, \quad (8)$$

we will make use of the following lemma.

Lemma 2 [4, Corollary (9.2.22)] *Let V be defined by (4) where $\text{meas}(\Gamma_2) > 0$. Then there exists a positive constant C such that*

$$\|\varepsilon(\mathbf{v})\|_{L^2(\Omega)} \geq C\|\mathbf{v}\|_{H^1(\Omega)} \quad \forall \mathbf{v} \in V.$$

As $\lambda > 0$ in (8), from Lemma 2 we have

$$\begin{aligned} b(\mathbf{v}, \mathbf{v}) &\geq 2\mu\|\varepsilon(\mathbf{v})\|_{L^2(\Omega)}^2 \\ &\geq 2\mu C^2\|\mathbf{v}\|_{H^1(\Omega)}^2. \end{aligned}$$

So we conclude that $b(\cdot, \cdot)$ is V -elliptic.

For the bilinear form $a(\cdot, \cdot)$ defined in (6), we have that

$$a(\mathbf{v}, \mathbf{v}) \geq 2\mu C^2\|\mathbf{v}\|_{H^1(\Omega)}^2 - \omega^2\rho\|\mathbf{v}\|_{L^2(\Omega)}^2,$$

and we deduce that $a(\cdot, \cdot)$ is V -coercive.

Because of Lemma 1 and assuming that $\beta_1 = \omega^2\rho$ is not an eigenvalue value of the problem, we conclude that (5) has a unique solution. Moreover, considering h small enough, by [9, Theorem 8.2.8] we achieve the uniqueness of solution of the discrete problem (7).

2.4 Deriving the numerical scheme in matrix form

The application of the finite element method invariably involves the solution of a sparse system of algebraic equations. In our proposal, that system in matrix form will be crucial to define the inverse problem.

Let us associate to each vertex x^j of the partition Ω_h in tetrahedra three base functions ϕ_{ji} , $j \in \{1, \dots, N\}$, $i \in \{1, 2, 3\}$. These functions are continuous in $\bar{\Omega}$ and linear in each tetrahedron, such that $\phi_{ji}(x^j) = 1$, $\phi_{ji}(x^k) = 0$ ($k \neq j$) and the support of ϕ_{ji} consists in all tetrahedra that share x^j as a vertex. We have

$$V_h = \text{span} \{ \phi_{11}, \dots, \phi_{N1}, \phi_{12}, \dots, \phi_{N2}, \phi_{13}, \dots, \phi_{N3} \}.$$

In this way, each component of the approximate solution $\mathbf{u}_h = (u_{1h}, u_{2h}, u_{3h}) \in V_h$ can be written as a linear combination of the basis functions ϕ_{ji} with

$$u_{ih}(x) = \sum_{j=1}^N U_{ji} \phi_{ji}(x), \quad i \in \{1, 2, 3\}, \quad (9)$$

where U_{ji} , $i \in \{1, 2, 3\}$, $j = \{1, \dots, N\}$, are the coefficients that we want to compute.

It should be noted that, if \mathbf{u}_h^* is the solution of the problem (7) then \mathbf{u}_h^* is the minimizer of the problem

$$J_h(\mathbf{v}_h) = \frac{1}{2}b(\mathbf{v}_h, \mathbf{v}_h) - l_{1,h}(\mathbf{v}_h), \quad \mathbf{v}_h \in V_h, \quad (10)$$

with

$$l_{1,h}(\mathbf{v}_h) = l(\mathbf{v}_h) + \omega^2 \rho(\mathbf{u}_h^*, \mathbf{v}_h). \quad (11)$$

Therefore the solution of finite elements \mathbf{u}_h^* satisfies

$$J_h(\mathbf{u}_h^*) = \min_{\mathbf{v}_h \in V_h} J_h(\mathbf{v}_h). \quad (12)$$

We can write problem (12) in matrix form as follows:

$$\text{find } V \in \mathbb{R}^{3N} \text{ such that } \chi(V) = \frac{1}{2}V^\top B^* V - V^\top F^* \text{ is minimum}, \quad (13)$$

where $V = [V_{11}, \dots, V_{N1}, V_{12}, \dots, V_{N2}, V_{13}, \dots, V_{N3}]^\top$, with B^* being the (global) $3N \times 3N$ stiffness matrix and F^* being a vector of dimension $3N \times 1$.

2.4.1 Reference tetrahedron

To calculate the global stiffness matrix B^* and the vector F^* of problem (13) we will make use of a reference tetrahedron.

For each tetrahedron K of the partition of Ω_h , consider $r_j^K = (x_j, y_j, z_j)$, $j \in \{1, \dots, 4\}$, representing the coordinates of its vertices in a global Cartesian's

system. We can write the coordinates of each point $r^K = (x, y, z)$ of K as a convex combination of the local coordinates (ξ, η, τ) (see Figure 1),

$$(x, y, z) = \sum_{j=1}^4 r_j^K \psi_j(\xi, \eta, \tau), \quad (14)$$

where

$$\begin{aligned} \psi_1(\xi, \eta, \tau) &= 1 - \xi - \eta - \tau, & \psi_2(\xi, \eta, \tau) &= \xi, \\ \psi_3(\xi, \eta, \tau) &= \eta, & \psi_4(\xi, \eta, \tau) &= \tau. \end{aligned}$$

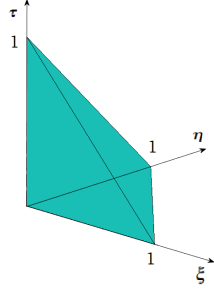


Fig. 1 Tetrahedron represented in local coordinates.

This transformation is associated with the Jacobi matrix which is given by $J_K = \frac{\partial(x, y, z)}{\partial(\xi, \eta, \tau)}$. The Jacobian can be written as

$$|J_K| = \det \begin{pmatrix} x_2 - x_1 & x_3 - x_1 & x_4 - x_1 \\ y_2 - y_1 & y_3 - y_1 & y_4 - y_1 \\ z_2 - z_1 & z_3 - z_1 & z_4 - z_1 \end{pmatrix} = \det \begin{pmatrix} x_1 & y_1 & z_1 & 1 \\ x_2 & y_2 & z_2 & 1 \\ x_3 & y_3 & z_3 & 1 \\ x_4 & y_4 & z_4 & 1 \end{pmatrix}.$$

Note that $|J_K| = 6|K|$, where $|K|$ is the volume of the tetrahedron K induced by r_1^K, \dots, r_4^K . So, for any continuous piecewise linear function $\mathbf{v}_h \in V_h$ and for $(x, y, z) \in K \subset \Omega_h$,

$$v_{ih}(x, y, z) = \sum_{j=1}^4 V_{ji} \psi_j(\xi, \eta, \tau), \quad i \in \{1, 2, 3\}, \quad (15)$$

where V_{ji} is the value of the function v_{ih} in the vertex of the tetrahedron K with position r_j^K , $i \in \{1, 2, 3\}$, $j \in \{1, \dots, 4\}$. The inverse $(J_K^T)^{-1} = \frac{(J_K^*)^T}{|J_K|}$ exists, where J_K^* is the adjugate matrix of J_K , and

$$\left(\frac{\partial v_{ih}}{\partial x} \quad \frac{\partial v_{ih}}{\partial y} \quad \frac{\partial v_{ih}}{\partial z} \right)^T = \frac{(J_K^*)^T}{|J_K|} \left(\frac{\partial v_{ih}}{\partial \xi} \quad \frac{\partial v_{ih}}{\partial \eta} \quad \frac{\partial v_{ih}}{\partial \tau} \right)^T, \quad i \in \{1, 2, 3\}. \quad (16)$$

We will use the relations in (16) to obtain the stiffness matrix B^* and the vector F^* .

2.4.2 Global matrix B^*

Let us compute the matrix B^* in (13). We will determine $b(\mathbf{v}_h, \mathbf{v}_h)$ in terms of the coefficients V_{ji} . Since the base functions are linear in each tetrahedron K then,

$$2\mu \|\varepsilon(\mathbf{v}_h)\|_{L^2(K)}^2 + \lambda \int_K (\nabla \cdot \mathbf{v}_h)^2 dx = |K| (2\mu \varepsilon(\mathbf{v}_h) : \varepsilon(\mathbf{v}_h) + \lambda (\nabla \cdot \mathbf{v}_h)^2).$$

Now let $\gamma(\mathbf{v}_h) = [\varepsilon_{11}(\mathbf{v}_h), \varepsilon_{22}(\mathbf{v}_h), \varepsilon_{33}(\mathbf{v}_h), 2\varepsilon_{12}(\mathbf{v}_h), 2\varepsilon_{13}(\mathbf{v}_h), 2\varepsilon_{23}(\mathbf{v}_h)]^\top$ where $\varepsilon_{ij}(\mathbf{v}_h) = \frac{1}{2} \frac{\partial v_{ih}}{\partial x_j} + \frac{1}{2} \frac{\partial v_{jh}}{\partial x_i}$, $i, j \in \{1, 2, 3\}$. It holds

$$2\mu \varepsilon(\mathbf{v}_h) : \varepsilon(\mathbf{v}_h) + \lambda (\nabla \cdot \mathbf{v}_h)^2 = \gamma^\top(\mathbf{v}_h) C \gamma(\mathbf{v}_h),$$

where the matrix C is given by

$$\begin{pmatrix} 2\mu + \lambda & \lambda & \lambda & 0 & 0 & 0 \\ \lambda & 2\mu + \lambda & \lambda & 0 & 0 & 0 \\ \lambda & \lambda & 2\mu + \lambda & 0 & 0 & 0 \\ 0 & 0 & 0 & \mu & 0 & 0 \\ 0 & 0 & 0 & 0 & \mu & 0 \\ 0 & 0 & 0 & 0 & 0 & \mu \end{pmatrix}. \quad (17)$$

Considering a 9×12 matrix P given by

$$P = \begin{pmatrix} 1 & 0 & 0 & 0 & 0 & 0 & 0 & 0 & 0 \\ 0 & 0 & 0 & 0 & 1 & 0 & 0 & 0 & 0 \\ 0 & 0 & 0 & 0 & 0 & 0 & 0 & 0 & 1 \\ 0 & 1 & 0 & 1 & 0 & 0 & 0 & 0 & 0 \\ 0 & 0 & 1 & 0 & 0 & 0 & 1 & 0 & 0 \\ 0 & 0 & 0 & 0 & 0 & 1 & 0 & 1 & 0 \end{pmatrix}$$

we have

$$\gamma(\mathbf{v}_h) = P \left[\frac{\partial v_{1h}}{\partial x_1}, \frac{\partial v_{1h}}{\partial x_2}, \frac{\partial v_{1h}}{\partial x_3}, \frac{\partial v_{2h}}{\partial x_1}, \frac{\partial v_{2h}}{\partial x_2}, \frac{\partial v_{2h}}{\partial x_3}, \frac{\partial v_{3h}}{\partial x_1}, \frac{\partial v_{3h}}{\partial x_2}, \frac{\partial v_{3h}}{\partial x_3} \right]^\top.$$

Let $V^K = [V_{11}, V_{21}, V_{31}, V_{41}, V_{12}, V_{22}, V_{32}, V_{42}, V_{13}, V_{23}, V_{33}, V_{43}]^\top$. Using (16), from (14) and (15) we obtain

$$\frac{\partial v_{ih}}{\partial \xi} = V_{2i} - V_{1i}, \quad \frac{\partial v_{ih}}{\partial \eta} = V_{3i} - V_{1i}, \quad \frac{\partial v_{ih}}{\partial \tau} = V_{4i} - V_{1i}, \quad i \in \{1, 2, 3\},$$

and then

$$\left(\frac{\partial v_{ih}}{\partial x} \quad \frac{\partial v_{ih}}{\partial y} \quad \frac{\partial v_{ih}}{\partial z} \right)^\top = \frac{1}{|J_K|} (J_K^*)^\top P_1 (V_{1i} \ V_{2i} \ V_{3i} \ V_{4i})^\top, \quad i \in \{1, 2, 3\} \quad (18)$$

being P_1 the matrix

$$P_1 = \begin{pmatrix} -1 & 1 & 0 & 0 \\ -1 & 0 & 1 & 0 \\ -1 & 0 & 0 & 1 \end{pmatrix}.$$

Therefore $\gamma(\mathbf{v}_h) = \frac{1}{|J_K|} P R^K V^K$, where R^K is a block matrix where each block diagonal is the matrix $(J_K^*)^\top P_1$.

As $|J_K| = 6 |K|$, we obtain

$$2\mu\varepsilon(\mathbf{v}_h) : \varepsilon(\mathbf{v}_h) + \lambda(\nabla \cdot \mathbf{v}_h)^2 = (V^K)^\top B^K V^K, \quad (19)$$

where

$$B^K = \frac{1}{36 |K|} (R^K)^\top P^\top C P R^K.$$

Note that matrix B^K is the local matrix corresponding to the tetrahedron of vertices r_1^K, \dots, r_4^K . We will construct B^* from these M local matrices. For the k -th tetrahedron K , let us consider an application L^K that is defined by a $N \times 4$ matrix with entries zeros and ones which identifies the vertices of K in the set of all vertices in Ω_h . The component (i, j) of L^K is one when the vertex with position r_j^K , $j \in \{1, \dots, 4\}$ is the i -th vertex in global numbering, $i \in \{1, \dots, N\}$. As we are working in \mathbb{R}^3 the idea is to do the same for the three components. It should be noted that

$$V^K = \begin{pmatrix} L^K & 0 & 0 \\ 0 & L^K & 0 \\ 0 & 0 & L^K \end{pmatrix}^\top V = (L_D^K)^\top V, \quad (20)$$

where L_D^K is a block matrix, where each block diagonal is the matrix L^K . With this relationship is possible to pass from $v_{ih}(r_j)$, $i \in \{1, 2, 3\}$, $j \in \{1, \dots, 4\}$, which are the values of the function \mathbf{v}_h in the local matrix vertices, to $v_{ih}(r_j)$, $i \in \{1, 2, 3\}$, $j \in \{1, \dots, N\}$ which are the values of the function for all vertices of the set Ω_h . So, rewriting (19) using (20), we obtain

$$(V^K)^\top B^K V^K = V^\top L_D^K B^K (L_D^K)^\top V$$

and therefore

$$b(\mathbf{v}_h, \mathbf{v}_h) = V^\top B^* V,$$

being $B^* = \sum_{K \in \Omega_h} L_D^K B^K (L_D^K)^\top$ the global stiffness matrix.

Note that B^* is symmetric since C given by (17) is symmetric and consequently B^K is also symmetric.

2.4.3 Vector F^*

Let us now compute the vector F^* in (13), such that $V^\top F^* = l_{1,h}(\mathbf{v}_h)$ with $l_{1,h}$ given by (11).

Let T_1, \dots, T_m be the set of all the triangles that define a face of one of the tetrahedrons of the partition which are contained in Γ_1 . The resulting subdivision (or mesh) is denoted by Γ_{1h} . So we can write

$$\int_{\Gamma_1} \mathbf{g} \cdot \mathbf{v}_h ds = \sum_{T \in \Gamma_{1h}} \int_T \mathbf{g} \cdot \mathbf{v}_h ds. \quad (21)$$

For each triangle T of the discretization of Γ_1 , let us consider the points $r_i^T = (x_i, y_i, z_i)$, $i \in \{1, 2, 3\}$ which correspond to the coordinates of its vertices. We assume that Γ_{1h} is contained in a surface with equation $z = S(x, y)$. Consider the local coordinates (ξ, η) where the vertices of the reference triangle are represented on the coordinate plane over the axes, as in Figure 2.

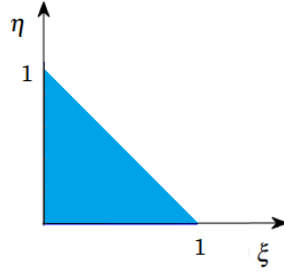


Fig. 2 Triangle represented in local coordinates.

In this form, we can write the coordinates of each point $r^T = (x, y, z)$ of T as a convex combination of the coordinates of the reference triangle

$$(x, y) = r_1 \varphi_1(\xi, \eta) + r_2 \varphi_2(\xi, \eta) + r_3 \varphi_3(\xi, \eta), \quad z = S(x, y), \quad (22)$$

where

$$\varphi_1(\xi, \eta) = 1 - \xi - \eta, \quad \varphi_2(\xi, \eta) = \xi, \quad \varphi_3(\xi, \eta) = \eta.$$

For this transformation, the Jacobi's matrix is given by

$$J_T = \frac{\partial(x, y)}{\partial(\xi, \eta)} = \begin{pmatrix} x_2 - x_1 & x_3 - x_1 \\ y_2 - y_1 & y_3 - y_1 \end{pmatrix}$$

and the Jacobian is

$$|J_T| = \det \begin{pmatrix} x_2 - x_1 & x_3 - x_1 \\ y_2 - y_1 & y_3 - y_1 \end{pmatrix} = \det \begin{pmatrix} x_1 & y_1 & 1 \\ x_2 & y_2 & 1 \\ x_3 & y_3 & 1 \end{pmatrix}.$$

Note that $|J_T| = 2|T|$ being $|T|$ the area of the triangle T defined by r_1^T, r_2^T, r_3^T .

For any continuous piecewise linear function $\mathbf{v}_h \in V_h$, and for $(x, y, z) \in T \subset \Gamma_{1h}$, we have that

$$v_{ih}(x, y, z) = \sum_{j=1}^3 V_{ji} \varphi_j(\xi, \eta), \quad z = S(x, y), \quad i \in \{1, 2, 3\}, \quad (23)$$

where V_{ji} is the value of the function v_{ih} in the vertex of the triangle T with position r_j^T , $i \in \{1, 2, 3\}$, $j \in \{1, 2, 3\}$.

Now we will consider that, for any triangle T , the points r_1^T, r_2^T, r_3^T correspond to the vertices V_1^T, V_2^T, V_3^T respectively. Consider the function \mathbf{g} in (21) defined in the triangle T written in terms of the local coordinates, as

$$g_i(x, y, z) = g_i \left(\frac{1}{3} \sum_{l=1}^3 V_l^T \right) \left(\sum_{p=1}^3 \varphi_p \right), \quad i \in \{1, 2, 3\}. \quad (24)$$

Therefore, by (23) and (24), we have

$$\int_T \mathbf{g} \cdot \mathbf{v}_h ds = |J_T| \sum_{1 \leq i, j \leq 3} \int_{\Delta_T} \left[g_i \left(\frac{1}{3} \sum_{l=1}^3 V_l^T \right) \left(\sum_{p=1}^3 \varphi_p \right) \right] V_{ji} \varphi_j d\xi d\eta, \quad (25)$$

where Δ_T defines the triangle in the local coordinates (ξ, η) , i.e.,

$$\Delta_T = \{(\xi, \eta) : 0 \leq \xi \leq 1, 0 \leq \eta \leq 1 - \xi\}.$$

We can summarize the last equality in the following matrix form

$$\int_T \mathbf{g} \cdot \mathbf{v}_h ds = |J_T| \sum_{i=1}^3 \int_{\Delta_T} [V_{1i}, V_{2i}, V_{3i}] D \begin{bmatrix} G_i \\ G_i \\ G_i \end{bmatrix} \quad (26)$$

where $G_i = g_i \left(\frac{1}{3} \sum_{l=1}^3 V_l^T \right)$, $i \in \{1, 2, 3\}$ and D is a 3×3 matrix where the component (i, j) is given by

$$\int_{\Delta_T} \varphi_i \varphi_j d\xi d\eta, \quad i, j \in \{1, 2, 3\}. \quad (27)$$

Note that in (27)

$$\int_{\Delta_T} \varphi_i^2 d\xi d\eta = \int_0^1 \int_0^{1-\xi} \varphi_i^2 d\eta d\xi = \frac{1}{12}, \quad i \in \{1, 2, 3\}$$

and

$$\int_{\Delta_T} \varphi_i \varphi_j d\xi d\eta = \int_0^1 \int_0^{1-\xi} \varphi_i \varphi_j d\eta d\xi = \frac{1}{24}, \quad i, j \in \{1, 2, 3\}, i \neq j.$$

Taking into account the previous expressions for the entries of the matrix D , we can write (26) as follows:

$$\int_T \mathbf{g} \cdot \mathbf{v}_h ds = |J_T| \sum_{i=1}^3 [V_{1i}, V_{2i}, V_{3i}, V_{4i}] D_1 \begin{bmatrix} G_i \\ G_i \\ G_i \\ 0 \end{bmatrix},$$

i.e., is the same as

$$(V^K)^\top D_2 G^T,$$

where $G^T = [G_1, G_1, G_1, 0, G_2, G_2, G_2, 0, G_3, G_3, G_3, 0]^\top$,

$$D_2 = |J_T| \begin{pmatrix} D_1 & 0 & 0 \\ 0 & D_1 & 0 \\ 0 & 0 & D_1 \end{pmatrix}, D_1 = \begin{bmatrix} D & 0_{3 \times 1} \\ 0_{3 \times 1}^\top & 0 \end{bmatrix}, D = \frac{1}{24} \begin{pmatrix} 2 & 1 & 1 \\ 1 & 2 & 1 \\ 1 & 1 & 2 \end{pmatrix}$$

and $0_{3 \times 1}$ is a 3×1 vector of zeros.

It should be noted that the expression in (20) is different for triangles. Instead of having the matrix L_D^K we will define another one, that is, L_D^T which is a block matrix where each diagonal block has a matrix of dimension $N \times 4$ with the fourth column being a vector of zeros. So for the triangles we obtain $V^K = (L_D^T)^\top V$.

Next, we present the calculation of the second term in (11). Consider that, for any tetrahedron K , the points $r_1^K, r_2^K, r_3^K, r_4^K$ correspond to the vertices $V_1^K, V_2^K, V_3^K, V_4^K$, respectively. The function \mathbf{u}_h^* defined in the tetrahedron K in terms of the local coordinates, can be written as

$$u_{ih}^*(x, y, z) = u_{ih}^* \left(\frac{1}{4} \sum_{l=1}^4 V_l^K \right) \left(\sum_{p=1}^4 \psi_p \right), i \in \{1, 2, 3\}.$$

So, by this approach and using (15) we have

$$\int_K \mathbf{u}_h^* \cdot \mathbf{v}_h dx = |J_K| \sum_{i=1}^3 \sum_{j=1}^4 \int_{\Delta_K} u_{ih}^* \left(\frac{1}{4} \sum_{l=1}^4 V_l^K \right) \left(\sum_{p=1}^4 \psi_p \right) V_{ji} \psi_j d\xi d\eta d\tau, \quad (28)$$

where Δ_K defines the tetrahedron in local coordinates (ξ, η, τ) , i.e.,

$$\Delta_K = \{(\xi, \eta, \tau) : 0 \leq \xi \leq 1, 0 \leq \eta \leq 1 - \xi, 0 \leq \tau \leq 1 - \xi - \eta\}.$$

This equality can be summarized in the following matrix form

$$\int_K \mathbf{u}_h^* \cdot \mathbf{v}_h dx = |J_K| \sum_{i=1}^3 [V_{1i}, V_{2i}, V_{3i}, V_{4i}] E \begin{bmatrix} U_i^* \\ U_i^* \\ U_i^* \\ U_i^* \end{bmatrix}, \quad (29)$$

where $U_i^* = u_{ih}^* \left(\frac{1}{4} \sum_{l=1}^4 V_l^K \right)$, $i \in \{1, 2, 3\}$ and E is a 4×4 matrix where the component (i, j) is given by

$$\int_{\Delta_K} \psi_i \psi_j d\xi d\eta d\tau, \quad i, j \in \{1, 2, 3, 4\}. \quad (30)$$

In (30),

$$\int_{\Delta_K} \psi_i^2 d\xi d\eta d\tau = \int_0^1 \int_0^{1-\xi} \int_0^{1-\xi-\eta} \psi_i^2 d\tau d\eta d\xi = \frac{1}{60}, \quad i \in \{1, \dots, 4\}$$

and

$$\int_{\Delta_K} \psi_i \psi_j d\xi d\eta d\tau = \int_0^1 \int_0^{1-\xi} \int_0^{1-\xi-\eta} \psi_i \psi_j d\tau d\eta d\xi = \frac{1}{120} \quad i \neq j.$$

Taking into account the previous expressions for the entries of the matrix E , we can write (29) as follows:

$$\int_K \mathbf{u}_h^* \cdot \mathbf{v}_h dx = (V^K)^\top B' (U^*)^K$$

where $(U^*)^K = [U_1^*, U_1^*, U_1^*, U_1^*, U_2^*, U_2^*, U_2^*, U_2^*, U_3^*, U_3^*, U_3^*, U_3^*]^\top$,

$$B' = |J_K| \begin{pmatrix} E & 0 & 0 \\ 0 & E & 0 \\ 0 & 0 & E \end{pmatrix} \quad \text{and} \quad E = \frac{1}{120} \begin{pmatrix} 2 & 1 & 1 & 1 \\ 1 & 2 & 1 & 1 \\ 1 & 1 & 2 & 1 \\ 1 & 1 & 1 & 2 \end{pmatrix}.$$

To compute the last integral in (11) it is enough to consider what has been done previously for the integrals over Ω . Therefore, we have that

$$\int_K \mathbf{f} \cdot \mathbf{v}_h dx = (V^K)^\top B' F^K$$

where $F^K = [F_1, F_1, F_1, F_1, F_2, F_2, F_2, F_2, F_3, F_3, F_3, F_3]^\top$.

Next, the purpose is to determine the explicit form of F^* . From (11) we have

$$l_{1,h}(\mathbf{v}_h) = \sum_{T \in \Gamma_{1h}} (V^K)^\top D_2 G^T + \sum_{K \in \Omega_h} (V^K)^\top B' \left[\omega^2 \rho (U^*)^K + F^K \right].$$

Then, using (20) results

$$l_{1,h}(\mathbf{v}_h) = V^T F^*$$

where

$$F^* = \sum_{T \in \Gamma_{1h}} L_D^T D_2 G^T + \omega^2 \rho \sum_{K \in \Omega_h} L_D^K B' (L_D^K)^\top U^* + \sum_{K \in \Omega_h} L_D^K B' F^K.$$

2.4.4 Linear system

We are now ready to write problem (13) as a linear system. Note that, by Section 2.3, the function χ has a unique minimizer V on \mathbb{R}^{3N} which satisfies $\nabla\chi(V) = 0$, where

$$\nabla\chi = \left(\frac{\partial\chi}{\partial V_{11}}, \dots, \frac{\partial\chi}{\partial V_{N1}}, \frac{\partial\chi}{\partial V_{12}}, \dots, \frac{\partial\chi}{\partial V_{N2}}, \frac{\partial\chi}{\partial V_{13}}, \dots, \frac{\partial\chi}{\partial V_{N3}} \right)^\top.$$

As B^* is symmetric, $\nabla\chi(V) = B^*V - F^*$ and the minimizer V of (13) satisfies $B^*V = F^*$. In this way, we calculate the coefficients U_{ji}^* , $i \in \{1, 2, 3\}$, $j \in \{1, \dots, N\}$ of (9) that allow to obtain the solution \mathbf{u}_h^* of the problem (7) which satisfy $B^*U^* = F^*$. This problem is equivalent to find U

$$U = [U_{11}, \dots, U_{N1}, U_{12}, \dots, U_{N2}, U_{13}, \dots, U_{N3}]^\top$$

such that

$$AU = F, \quad (31)$$

where

$$A = B^* - \omega^2 \rho \sum_{K \in \Omega_h} L_D^K B' (L_D^K)^\top$$

and

$$F = \sum_{T \in \Gamma_{1h}} L_D^T D_2 G^T + \sum_{K \in \Omega_h} L_D^K B' F^K.$$

3 Inverse problem

3.1 Description of the inverse problem

In this section we mathematically define the inverse problem, which can be described by the following minimization program:

$$\begin{aligned} \min_{\mu, \lambda} & \|AU_{obs} - F\|_{L_h^2(\Omega)} \\ \text{s.t.} & \quad \mu \in [\mu_1, \mu_2] \\ & \quad \lambda \in [\lambda_1, \lambda_2] \end{aligned} \quad (32)$$

where A and F define the linear system to solve the direct problem (31) and U_{obs} is the vector that contains the information of the given data. Here we use the discrete L_h^2 -norm, defined for any $3N \times 1$ vector y , as

$$\|y\|_{L_h^2(\Omega)}^2 = \sum_{K \in \Omega_h} \|y\|_{L_h^2(K)}^2,$$

with

$$\|y\|_{L_h^2(K)}^2 = \frac{|K|}{4} \sum_{i=1}^4 \sum_{j=0}^2 y_{t(r_i^K) + jN}^2,$$

where $|K|$ denotes the volume of the tetrahedron K with vertices $r_i^K, i \in \{1, \dots, 4\}$. The function t is defined by

$$\begin{aligned} t : \mathbb{R}^3 &\rightarrow \{1, \dots, N\} \\ r_i^K &\mapsto t(r_i^K), \end{aligned}$$

where $t(r_i^K)$ is the index that corresponds to vertex of r_i^K in the global numbering.

The constraint $(\mu, \lambda) \in [\mu_1, \mu_2] \times [\lambda_1, \lambda_2]$ in (32) ensures a range of values for μ and λ compatible with the biological structures.

For convenience we denote the objective function by l ,

$$l(\mu, \lambda) = \|AU_{obs} - F\|_{L_h^2(\Omega)}^2, \quad (33)$$

and define the unconstrained minimization problem

$$\min_{\mu, \lambda} l(\mu, \lambda). \quad (34)$$

3.2 Hessian matrix and convexity

A natural question that arises is whether the function l is convex or not. For that purpose, let us check the corresponding hessian. We start by deriving the expressions of the first-order partial derivatives in order to μ and λ . We have that

$$\frac{\partial l}{\partial \mu}(\mu, \lambda) = \sum_{K \in \Omega_h} \frac{|K|}{4} \sum_{i=1}^4 \sum_{j=0}^2 \frac{\partial}{\partial \mu} \left[(AU_{obs} - F)_{t(r_i^K)+jN}^2 \right]. \quad (35)$$

Since

$$\frac{\partial}{\partial \mu} \left[(AU_{obs} - F)_{t(r_i^K)+jN}^2 \right] = 2(AU_{obs} - F)_{t(r_i^K)+jN} \left(\frac{\partial A}{\partial \mu} U_{obs} \right)_{t(r_i^K)+jN},$$

(35) can be written in the form

$$\frac{\partial l}{\partial \mu}(\mu, \lambda) = \sum_{K \in \Omega_h} \frac{|K|}{2} \sum_{i=1}^4 \sum_{j=0}^2 (AU_{obs} - F)_{t(r_i^K)+jN} \left(\frac{\partial A}{\partial \mu} U_{obs} \right)_{t(r_i^K)+jN}.$$

Let \mathbb{I} be a $1 \times M$ vector with all entries equal to one, $\text{diag}(\frac{|K|}{2})$ the diagonal matrix of size $M \times M$ with entries $\frac{|K_j|}{2}, j \in \{1, \dots, M\}$ for some numbering of the tetrahedra, $\text{diag}(AU_{obs} - F)$ the diagonal matrix of size $3N \times 3N$ with entries $(AU_{obs} - F)_{t(r_i^K)+jN}$ and $\mathbf{\Lambda} = [\mathbf{\Lambda}, \mathbf{\Lambda}, \mathbf{\Lambda}]$ a $M \times 3N$ matrix where $\mathbf{\Lambda}$ is a $M \times N$ matrix with entries $\delta_{ji} = 1$ if and only if the vertex $r_i^K \in K_j$ and $\delta_{ji} = 0$ otherwise.

In this way, we can write

$$\frac{\partial l}{\partial \mu}(\mu, \lambda) = \mathbb{I} \text{diag}\left(\frac{|K|}{2}\right) \mathbf{\Lambda} \text{diag}(AU_{obs} - F) \frac{\partial A}{\partial \mu} U_{obs}.$$

Similarly, we obtain the expression for the first-order derivative in order to λ ,

$$\frac{\partial l}{\partial \lambda}(\mu, \lambda) = \mathbb{I} \operatorname{diag}\left(\frac{|K|}{2}\right) \mathbf{\Lambda} \operatorname{diag}(AU_{obs} - F) \frac{\partial A}{\partial \lambda} U_{obs}.$$

Next, we will derive the expression of the second-order partial derivative in order to μ . Taking into account that the second order derivative of the matrix A in order to μ is zero, then we obtain

$$\frac{\partial^2 l}{\partial \mu^2}(\mu, \lambda) = \mathbb{I} \operatorname{diag}\left(\frac{|K|}{2}\right) \mathbf{\Lambda} \operatorname{diag}\left(\frac{\partial A}{\partial \mu} U_{obs}\right) \frac{\partial A}{\partial \mu} U_{obs}.$$

In a similar way, we derive the expression for the second-order partial derivative of l in order to λ ,

$$\frac{\partial^2 l}{\partial \lambda^2}(\mu, \lambda) = \mathbb{I} \operatorname{diag}\left(\frac{|K|}{2}\right) \mathbf{\Lambda} \operatorname{diag}\left(\frac{\partial A}{\partial \lambda} U_{obs}\right) \frac{\partial A}{\partial \lambda} U_{obs}$$

and for the mixed derivative we get

$$\frac{\partial^2 l}{\partial \lambda \partial \mu}(\mu, \lambda) = \mathbb{I} \operatorname{diag}\left(\frac{|K|}{2}\right) \mathbf{\Lambda} \operatorname{diag}\left(\frac{\partial A}{\partial \lambda} U_{obs}\right) \frac{\partial A}{\partial \mu} U_{obs}.$$

Let (μ_0, λ_0) be any point in the domain of l , that is, $(\mu_0, \lambda_0) \in [\mu_1, \mu_2] \times [\lambda_1, \lambda_2]$. Note that function l can be represented in the following quadratic form:

$$l(\mu, \lambda) = l(\mu_0, \lambda_0) + \nabla l(\mu_0, \lambda_0)^\top \Delta_{\mu_0 \lambda_0} + \frac{1}{2} \Delta_{\mu_0 \lambda_0}^\top H \Delta_{\mu_0 \lambda_0}, \quad (36)$$

where $\Delta_{\mu_0 \lambda_0} = [\mu - \mu_0, \lambda - \lambda_0]^\top$ and H is the hessian constant matrix.

Lemma 3 *The hessian matrix of l is positive semidefinite.*

Proof Writting

$$\frac{\partial A}{\partial \mu} U_{obs} = (a_i)_{1 \leq i \leq 3N} \quad \text{and} \quad \frac{\partial A}{\partial \lambda} U_{obs} = (b_i)_{1 \leq i \leq 3N},$$

for some constants a_i and b_i , $i \in \{1, \dots, 3N\}$, we can express the second-order partial derivatives in the form

$$\frac{\partial^2 l}{\partial \mu^2}(\mu, \lambda) = \sum_{i=1}^{3N} c_i a_i^2, \quad \frac{\partial^2 l}{\partial \lambda^2}(\mu, \lambda) = \sum_{i=1}^{3N} c_i b_i^2$$

and

$$\frac{\partial^2 l}{\partial \lambda \partial \mu}(\mu, \lambda) = \sum_{i=1}^{3N} c_i a_i b_i,$$

where c_i , $i \in \{1, \dots, 3N\}$, are non-negative constants.

Let H be the hessian matrix of l . We can easily observe that the diagonal components of H , $\frac{\partial^2 l}{\partial \mu^2}(\mu, \lambda)$ and $\frac{\partial^2 l}{\partial \lambda^2}(\mu, \lambda)$, are non-negative constants. Let us now prove that the determinant of H is non-negative, that is

$$\det H = \frac{\partial^2 l}{\partial \mu^2}(\mu, \lambda) \frac{\partial^2 l}{\partial \lambda^2}(\mu, \lambda) - \left(\frac{\partial^2 l}{\partial \lambda \partial \mu}(\mu, \lambda) \right)^2 \geq 0.$$

We conclude that

$$\sum_{i=1}^{3N} c_i a_i^2 \sum_{i=1}^{3N} c_i b_i^2 - \left(\sum_{i=1}^{3N} c_i a_i b_i \right)^2 = \sum_{i,j=1, i \neq j}^{3N} c_i c_j (a_i b_j - a_j b_i)^2 \geq 0.$$

Since l is a quadratic function and the hessian of the function l is a 2 by 2 positive semidefinite matrix then, if $\det H \neq 0$, the Newton's method applied to (34) converges to a solution s in one iteration which is given by

$$s = s_0 - H^{-1} \nabla l(s_0)$$

where $s_0 = (\mu_0, \lambda_0)^T \in \mathbb{R}^2$ is any initial guess. If the unconstrained problem solution s checks the constraints of the problem (32), then it is the optimal solution of (32). Otherwise, it is necessary to determine the optimal solution along the active constraints, which is again a quadratic problem.

4 Computational results

In this section we present some computational results. In the context of a real application, data is affected by noise. Here, we performed experiments with noise free data as well as noisy data in order to assess the sensitivity of our method to noise.

Let us consider the objective function defined by (33), which corresponds to the following setting: $\Omega = [-2, 2]^3$ with $\partial\Omega = \Gamma_1 \cup \Gamma_2$ where Γ_1 is the face of the cube contained in the plane $z = -2$; the mesh is a partition of Ω into 48 tetrahedrons; $\rho = 1$, $w = 2\pi \times 10^6$, the functions \mathbf{g} , \mathbf{f} are defined respectively by $g_i = 5.86 \times 10^{-3}$ and $f_i = 0$, $i \in \{1, 2, 3\}$.

To illustrate the performance of the proposed method we used fabricated data obtained by simulating the direct problem. In particular, we considered U_{obs} as the solution of (31) with $E = 4.66 \times 10^6$ and $\nu = 0.45$ [8]. In this way, $(\mu, \lambda) = (1.6069 \times 10^6, 1.4462 \times 10^7)$ is the optimal solution of the inverse problem. For the optimization problem we choose the set $I = [0.9\mu, 1.1\mu] \times [0.9\lambda, 1.1\lambda]$ and the surface of the objective function l defined in I is presented in Figure 3. Considering this setting, we performed several simulations using different starting points and we always recovered the exact solution.

Let us now check the robustness of the proposed method when considering noisy data. To put this idea in practice, we consider gaussian noise $R \sim N(0, \sigma)$ where R is a vector of dimension $3N \times 1$ and σ is the standard deviation. So

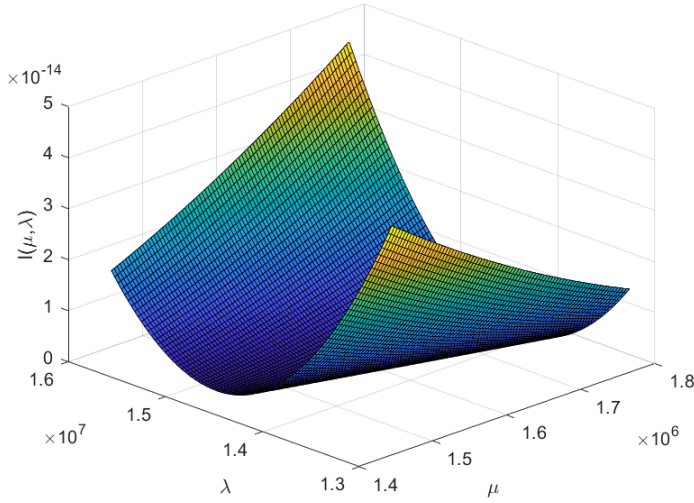


Fig. 3 Surface of the objective function l in I .

instead U_{obs} , we consider as data $\bar{U}_{obs} = (R + 1_{3N \times 1})U_{obs}$, where $1_{3N \times 1}$ is a $3N \times 1$ vector with all components equal to one and the i -th component of the vector \bar{U}_{obs} is given by $(R(i) + 1)U_{obs}(i)$, $i \in \{1, \dots, 3N\}$. We consider variations of σ in the set $\{0, 10^{-8}, 10^{-7}, 10^{-6}, 10^{-5}\}$ and, for each value of σ , we consider simulations with 30 random initial points. We only consider one iteration of the Newton's method for each initial solution.

Figure 4 presents the relative error average obtained from thirty simulations for each value of σ .

The results are according to the expectations as the relative error grows with the level of noise. For small values of the standard deviation σ the optimal solution is well recovered.

Declarations

Competing interests: The authors declare no conflict of interest. **Author's contributions:** Conceptualization, S.B., R.H. and J.L.S.; methodology, S.B. and R.H.; formal analysis, S.B. and R.H.; software, R.H.; validation, S.B., R.H. and J.L.S.; supervision, S.B., writing original draft preparation, R.H.; writing-review and editing, S.B., R.H. and J.L.S.. All authors have read and agreed to the published version of the manuscript. **Availability of data:** The code supporting the conclusions of this manuscript will be made available by the authors upon formal and reasonable request.

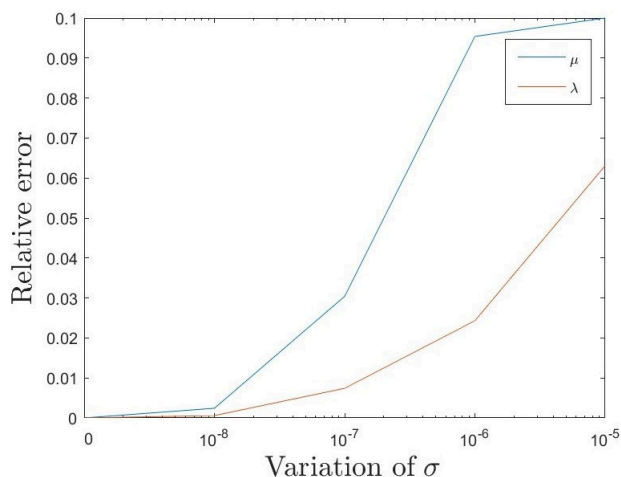


Fig. 4 Relative error average obtained from thirty simulations for each value of σ

Funding

This work was partially supported by the Centre for Mathematics of the University of Coimbra (funded by the Portuguese Government through FCT/MCTES, DOI 10.54499/UIDB/00324/2020); the FEDER Funds through the Operational Program for Competitiveness Factors - COMPETE and by Portuguese National Funds through FCT - Foundation for Science and Technology "2021.06672.BD"; the FCT (Portugal) research project PTDC/EMD-EMD/32162/2017, COMPETE and Portugal 2020.

References

1. M. Ainsworth, C. Parker. Unlocking the secrets of locking: Finite element analysis in planar linear elasticity. *Computer Methods in Applied Mechanics and Engineering*, 395, 2022.
2. S. Barbeiro, P. Serranho. The method of fundamental solutions for the direct elastography problem in the human retina. *Proceedings of the 9th Conference on Trefftz Methods and 5th Conference on Method of Fundamental Solutions*, Springer, 2020.
3. S. Barbeiro, R. Henriques, J. Santos. The derivative free trust-region method for the inverse elastography problem. Accepted to *Proceedings of the 22nd ECMI Conference on Industrial and Applied Mathematics*, Springer, 2023.
4. S. C. Brenner, L. R. Scott. *The mathematical theory of finite element methods*. Springer, 1997.
5. C. Carstensen, G. Dolzmann, S.A. Funken, D.S. Helm, Locking-free adaptive mixed finite element methods in linear elasticity. *Computer Methods in Applied Mechanics and Engineering*, 190 (13–14), 1701-1718, 2000.
6. D. Claus, M. Mlikota, J. Geibel, T. Reichenbach, G. Pedrini, J. Mischinger, S. Schmauder, and W. Osten. Large-field-of-view optical elastography using digital image correlation for biological soft tissue investigation. *Journal of Medical Imaging*, 4 (1): 1–14, 2017.
7. M. M. Doyley. Model-based elastography: a survey of approaches to the inverse elasticity problem. *Physics in Medicine and Biology*, 57 (3):R35-R73, 2012.
8. G. Giannakoulas, G. Giannoglou, J. Soulis, T. Farmakis, S. Papadopoulou, G. Parcharidis, G. Louridas. *A computational model to predict aortic wall stresses in patients with systolic arterial hypertension*. Elsevier, *Medical Hypotheses*, 2005.

9. W. Hackbusch. Elliptic differential equations. Theory and Numerical Treatment, 1992.
10. B. F. Kennedy, X. Liang, S. G. Adie, D. K. Gerstmann, B. C. Quirk, S. A. Boppart, and D. D. Sampson. In vivo three-dimensional optical coherence elastography. *Opt. Express*, 19 (7):6623–6634, 2011.
11. E. Park, A.M. Maniatty. Shear modulus reconstruction in dynamic elastography: time Harmonic case. *Phys. Med. Biol.* 51(15), 3697-3721, 2006.
12. Y. Qu, Y. He, Y. Zhang, T. Ma, J. Zhu, Y. Miao, C. Dai, M. Humayun, Q. Zhou, and Z. Chen. Quantified elasticity mapping of retinal layers using synchronized acoustic radiation force optical coherence elastography. *Biomed.Opt.Express*, 9 (9):4054–4063, 2018.
13. P. Serranho, S. Barbeiro, R. Henriques, A. Batista, M. Santos, C. Correia, J. Domingues, C. Loureiro, J. Cardoso, R. Bernardes, M. Morgado. On the numerical solution of the inverse elastography problem for time-harmonic excitation. In *Proceedings of the 2nd International Conference on Image Processing and Vision Engineering (IMPROVE 2022)*, pages 259-264, 2022.
14. J. Zhu, Y. Miao, L. Qi, Y. Qu, Y. He, Q. Yang, and Z. Chen. Longitudinal shear wave imaging for elasticity mapping using optical coherence elastography. *Applied Physics Letters*, 110 (20):201101, 2017.